Volume 3, Number 10 ACTA PHYSICA SINICA October, 1994
1004-423X/94/03100746-12 (Overseas Edition)

BEHAVIOR OF Ar PLASMA FORMED IN A HIGH DENSITY PLASMA SOURCE–AN ECR REACTOR*

WU HAN-MING(吴汉明), D.B. GRAVES,† R.K PORTEOUS,‡ and LI MING(李 明)
Institute of Mechanics, Academia Sinica, Beijing 100080, China; and China Center of Advanced Science and Technology (World Laboratory), P.O. Box 8730, Beijing 100080, China
†*Department of Chemical Engineering, University of California, Berkeley CA94720, U.S.A.*
‡*Plasma Research Laboratory, Australia National University, Canberra, Australia.*

(Received 7 December 1993)

In order to develop the ultra-large scale integration(ULSI), low pressure and high density plasma apparatus are required for etching and deposit of thin films. To understand critical parameters such as the pressure, temperature, electrostatic potential and energy distribution of ions impacting on the wafer, it is necessary to understand how these parameters are influenced by the power input and neutral gas pressure. In the present work, a 2-D hybrid electron fluid-particle ion model has been developed to simulate one of the high density plasma sources–an Electron Cyclotron Resonance (ECR) plasma system with various pressures and power inputs in a non-uniform magnetic field. By means of numerical simulation, the energy distributions of argon ion impacting on the wafer are obtained and the plasma density, electron temperature and plasma electrostatic potential are plotted in 3-D. It is concluded that the plasma density depends mainly on both the power input and neutral gas pressure. However, the plasma potential and electron temperature can hardly be affected by the power input, they seem to be primarily dependent on the neutral gas pressure. The comparison shows that the simulation results are qualitatively in good agreement with the experiment measurements.

PACC: 5265

I. INTRODUCTION

As a kind of high density plasma source, electron cyclotron resonance (ECR) plasma source is now becoming widely studied for etching and thin-film deposit in microelectronics industry.[2–8] Geometrically, there are two main types of ECR apparatuses. The first type is the so called extended tool that is widely used in scientific research because in such an apparatus there are a lot of space so that it can be conveniently used for diagnosis and the wafer position can be moved around. The other type is the so called compact tool that is proposed by some scientists.[9–12] The major advantage of the compact configuration is its efficiency. Some commercial products of Japanese ECR are made in the compact configurations.In the present paper, our attention is only focused on the former one.

One of the simplest types uses an Ar plasma.[2,5] The interesting use of ECR system for etching research requires the study of the plasma properties as a function of various system parameters, for example, microwave power input and neutral gas pressure. To interpret the results of such studies, it seems interesting to find, for a certain ECR geometry, how

*Project supported in part by the Presidential Foundation of the Chinese Academy of Sciences.

the plasma density is sensitive to the power input and the neutral gas pressure parameters, and what is the relationship between the electron temperature, electrostatic potential and pressure as well as power input.

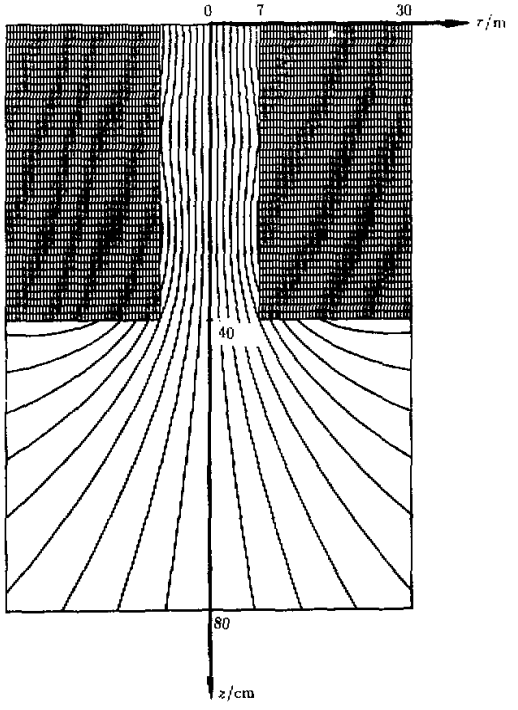

Fig. 1. The schematic of ECR plasma chamber and magnetic flux configuration.

In the present work, using a two-dimensional (2-D) numerical method, we simulate the argon plasma behaviors in an extended ECR system in a non-uniform magnetic field induced by eight coil sets outside the chamber. The geometry of the ECR chamber is the same as that made by Stevens of Princeton University.[4] In cylindrical co-ordinates (r, z, θ), let the origin be at the top center of the chamber. It is supposed to be axial symmetric, i.e., $\frac{\partial}{\partial\theta} = 0$. The inner radius of the coil is 12 cm and the outer one 16 cm. The top coils carry 150 A current and the other ones 140 A. The axial positions of the coils are $z = -2$, 5, 25 and 32 cm. The source is of 40 cm length with a diameter 15 cm, and the down stream chamber is of 40 cm length with a radius 30 cm. The magnetic fluxes inside the chamber are plotted in Fig. 1. The magnetic field on the z-axis is displayed in Fig. 2. The frequency of the microwave is 2.45 GHz. The power input can be set 0.6, 1 and 2 kW for different cases.

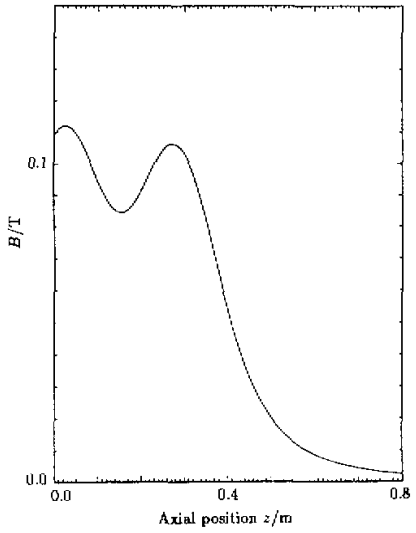

Fig. 2. The magnetic field on the z-axis. The resonance zone is at z=10 cm for B_0=950 G. The magnetic field decays rapidly in downstream and it is only about 20 G on the bottom (z=80 cm).

II. ASSIMPTIONS AND MATHEMATICAL MODEL

A hybrid electron fluid-particle ion model with two-dime-nsional space and three-dimensional velocity ($2D3V$) is adopted. According to Stevens' work[3], we assume the resonant magnetic field B_0=950 G with 25 G width. The neutral gas pressure and temperature are set to be uniform, and the plasma is primarily formed by ionization in the source chamber. The microwave power input is totally absorbed by those electrons in the resonant zone, and power deposition profile is

$$P_{\rm ecr} = c\frac{1-(r/a)^4}{1+[(B-B_0/0.0025)]^2}\,, \tag{1}$$

where a is the radius of the source chamber, r radial position, B magnetic field and c a constant, determined by normalization of total power input. From Fig. 2, it is found that near z = 10 cm there is the resonant zone where all of the microwave power are supposed to be transferred to the electrons. Since the treatments of electrons and ions are completely different, the subject will be discussed in the following separated parts.

A. Electron equations

The electrons in a plasma can be treated as a fluid even when the neutral pressure

is quite low. The principal random collision is electron-electron Coulomb collision. It is known that ECR requires that the ratio of electron-neutral gas collision frequency to electron cyclotron frequency be small, i.e., $\nu_{eo}/\omega_{ce} << 1$. In addition, the diffusion relation of the perpendicular component (perpendicular to magnetic line) and parallel component is

$$\mu_\perp = \frac{\nu_{eo}^2}{\nu_{eo}^2 + \omega_{ce}^2}\mu_\parallel .$$

It is obvious that the parallel component $\mu_\parallel$ is much greater than $\mu_\perp$ in a typical ECR parameter range. For example, if temperature T_e=3 eV, pressure $p = 1$ Pa and magnetic field $B = 10$ G, then there should be $\mu_\perp/\mu_\parallel = 0.02$. Therefore, the mobility of the perpendicular component can always be neglected in typical ECR systems. Thus we set $\mu = \mu_\parallel = e/m_e\nu_{eo}$, where e is the elementary charge.

One of the main inelastic collision processes is ionization. In the steady state, for argon plasma, the ratio of electron-electron collision frequency to electron-neutral gas collision frequency ν_{ee}/ν_{eo} is about 10^3 when $p = 1$ Pa, $T_e = 3$ eV and electron density $n_e = 10^{18}$. So it seems reasonable to assume that the electron velocity distribution be close to Maxwellian. This assumption is proved to be reasonable by experimental measurements.[14] The governing equations for electron fluid are written as

$$\nabla \cdot \boldsymbol{\varphi} = n_e \nu_i(T_e) , \tag{2}$$

$$\boldsymbol{\varphi} = \boldsymbol{\mu} : [n_e \nabla\phi - \nabla(n_e T_e)] , \tag{3}$$

$$\boldsymbol{Q} = 2eT_e(\boldsymbol{\varphi} - n_e \boldsymbol{\mu} : \nabla T_e) , \tag{4}$$

$$\nabla \cdot \boldsymbol{Q} = n_e P_{ecr} + e\boldsymbol{\varphi} \cdot \nabla\phi - P_{loss} , \tag{5}$$

where the right side of Eq. (2) is the mass source term, which creates all electrons and ions, i.e., the so called creation rate; n_e, ν_i, $\boldsymbol{\varphi}$, ϕ, and $\boldsymbol{Q}$ are the electron density, the ionization frequency, the electron flux, the plasma electrostatic potential, and the electron energy flux, respectively. The definition of the power consumption is

$$P_{loss} = P_i + P_x + P_m + P_{el} ,$$

where P_i, P_x, P_m and P_{el} are the power consumptions for ionization, excitation, metastable excitation and elastic-neutral collision, respectively.

Poisson's equation makes the system of equations closed by giving a relation between the local electrostatic potential and the electron and ion charge densities,

$$\varepsilon_0 \nabla^2\phi = e(n_e - n_i) , \tag{6}$$

where n_i is ion density and ε_0 the dielectric constant.

B. Ion equations

The ions are considered as particles in the present work. The total number of the particles is 20,000 to 100,000. Each particle, the so called meta-ion, presents many real ions. The dynamics of each meta-ion is still that of real ions. However, in fluid density each meta-ion represents a large number N_s of real ions. Usually, N_s is of the order of 10^{10} to 10^{12} in the simulation. Only in the steady state is N_s a constant.

The dynamic algorithm takes the position (r, z) and the velocity (v_r, v_z, v_θ) of a particle and calculates its new position in phase space after the particle travels a time step Δt. For convenience, the cylindrical co-ordinates (r, z, θ) are transformed to (R, Z, θ), where $R = r^2, Z = z$. By means of partial derivatives of Lagrangian

$$L = \frac{m}{2}(\dot{Z}^2 + \dot{R}^2/4R + R\dot{\theta}^2) - e\phi + e\sqrt{R}A_\theta\dot{\theta} ,$$

the following three equations of motion can be obtained:

$$\ddot{Z} = \frac{\delta\Phi}{\delta Z} + \frac{\delta\Psi}{\delta Z} , \tag{7}$$

$$\ddot{R} = \frac{\dot{R}^2}{2R} + 2R\dot{\theta}^2 + 4R\frac{\delta\Phi}{\delta R} + 4R\frac{\delta\Psi}{\delta R}\dot{\theta} , \tag{8}$$

$$\frac{\mathrm{d}}{\mathrm{dt}}(R\dot{\theta} + \Psi) = 0 , \tag{9}$$

where the dot operator denotes the derivative with respect to time, m is an argon ion mass, $\Phi = -e\phi/m$ the electrostatic potential, and $\Psi = erA_\theta/m$ the magnetic flux. From Eq. (9), it is shown that the canonical angular momentum $P = R\dot{\theta} + \Psi$ is a constant of the motion.

C. Boundary conditions

In our simulation, the plasma sheath is assumed to be infinitesimally thin and the electrostatic potential discontinuity $\Delta\phi = \phi_s - \phi_w$ is defined as the difference between the plasma potential at the sheath edge ϕ_s and the wall potential ϕ_w. There are two kinds of boundary conditions in an ECR apparatus.

The first kind is of conducting walls, where the wall potential ϕ_w is specified externally. Since the electrons are assumed to have Maxwellian velocity distribution, the electron flux on the boundary should be

$$\varphi_{ew} = \frac{1}{4}n_e\langle v_{th}\rangle \exp(\frac{\Delta\phi}{T_e}) , \tag{10}$$

where $\langle v_{th} \rangle$ is an average thermo-velocity. In an analogous way, the energy flux of the electrons is represented by

$$Q_{ew} = \frac{e}{2} n_e \langle v_{th} \rangle T_e \exp(\frac{\triangle \phi}{T_e}) . \tag{11}$$

The second kind of the boundary is of dielectric wall, where the surface potential will float with respect to ground. The ion flux φ_{iw} is specified to determine ϕ_w at each grid point of boundary, i.e., from $\varphi_{iw} = \varphi_{ew}$ and Eq. (10). Therefore, the wall potential would be

$$\phi_w = \phi_s + T_e \ln \frac{4\varphi_{iw}}{n_e \langle v_{th} \rangle} . \tag{12}$$

Although not included in the present paper, a thin sheath approximation is proved to be possible for rf bias surface, especially for low bias power. The detailed discussion of the rf bias will be provided in another paper in the future.

III. NUMERICAL RESULTS AND DISCUSSIONS

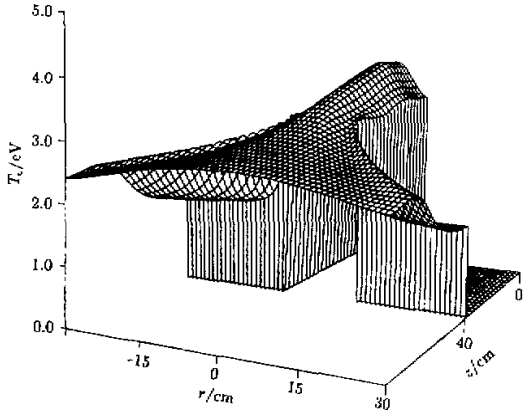

Fig. 3. The spatial distribution of the electron temperature. $p = 1$ mTorr and $P = 0.6$ kW.

Using elliptical integral's definition, we obtain the magnetic configuration (see Fig. 1). The coil positions and coil currents are predetermined. The magnetic field on the z-axis is shown in Fig. 2, from which it is found that the resonant zone is located at about $z = 0.1$ m if the result of Ref [4] is taken into account.

In the simulation, three neutral gas pressures are presumed, i.e., $p = 1$, 2 and 5 mTorr, and the microwave power inputs are given as $P = 0.6$, 1 and 2 kW. In Fig. 3 through Fig. 6, the spatial distributions of the plasma density n, the electron temperature T_e and the electrostatic potential in plasma ϕ are displayed for the case of $p = 1$ mTorr and $p = 0.6$ kW. One can see that all of them have their maximum values near the resonant zone ($r = 0, z = 10$ cm).

In Fig. 3, it is found that the electron temperature distribution is quite flat. The difference between the maximum and the minimum values is only about 1.5 eV. This is because the electron mobility is very large and their energy transport becomes quite fast.

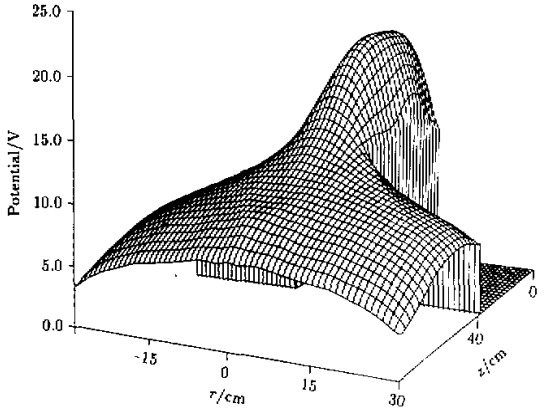

Fig. 4. The spatial distribution of the plasma electrostatic potential. $p = 1$ mTorr and $P = 0.6$ kW.

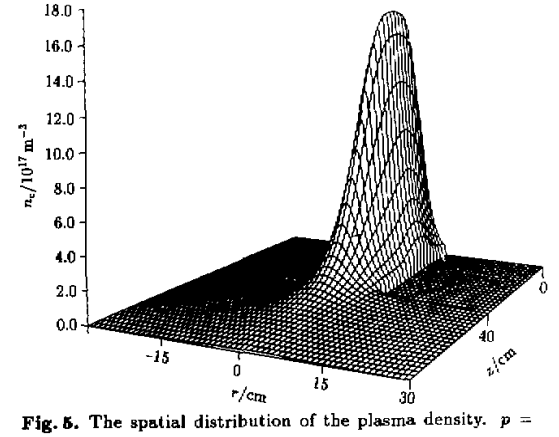

Fig. 5. The spatial distribution of the plasma density. $p =$ 1 mTorr and $P = 0.6$ kW.

From Fig. 4, it is found that the plasma potential distribution near the bottom is about 5 to 9 V. Without an applied bias, the ions impacting on the wafer would carry the kinetic energy of 5 to 9 eV. Figure 5 shows the plasma density distribution. It is obvious that the density gradient is very large especially in the radial direction in the source chamber. The maximum value reaches to $1.8 \times 10^{18}\,m^{-3}$ near the resonant area and the minimum one is only $2 \times 10^{17}\,m^{-3}$ at the edge of the source chamber ($r = 7.5$ cm, $z < 40$ cm). Therefore, it can be understood that only when there is a strong magnetic field, can the plasma density have such a large density gradient. The farther away the distance from the plasma source, the lower the density and the more uniform the distribution of density in the radial direction. That is why some scientists believe that the etching uniformity depends primarily on how far the wafer is from the ECR plasma source.[7] Conventionally, one has to sacrifice etching rate to get the necessary etching uniformity. However, recently it has been proved that it

may be possible to get a better uniformity without the loss of etching rate, i.e., optimizing either the power deposit profile or the magnetic configuration. That is why the commercial compact ECR etching tool works fairly well on the uniformity problem. We have discussed this matter in another paper.[12]

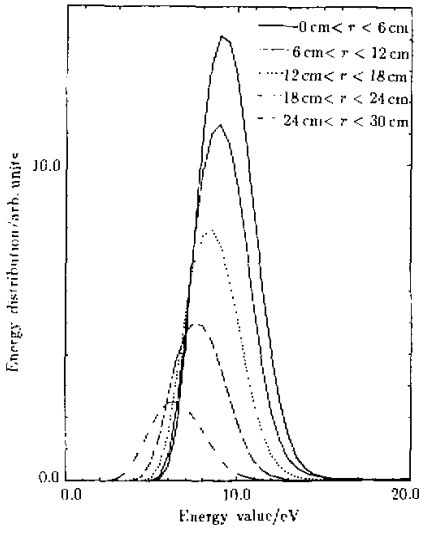

Fig. 6. The energy distributions of the ions impacting on the wafer. p = 1 mTorr and P = 0.6 kW.

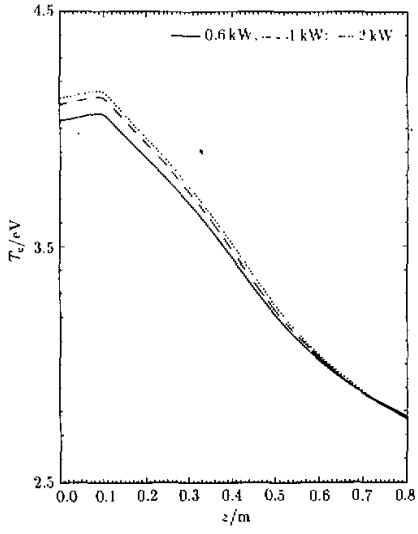

Fig. 7. The electron temperature distributions on the z-axis for different power inputs at p = 1 mTorr.

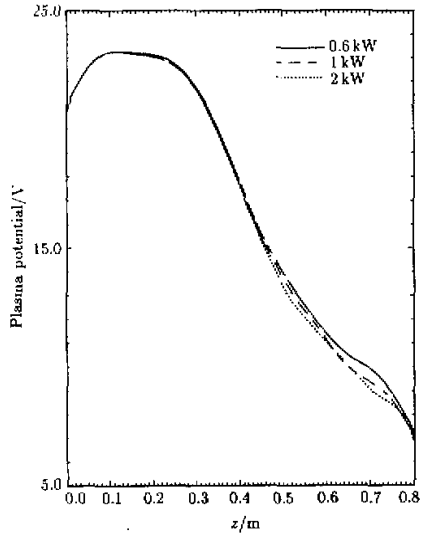

Fig. 8. The plasma potentials on the z-axis for different power inputs at p = 1 mTorr.

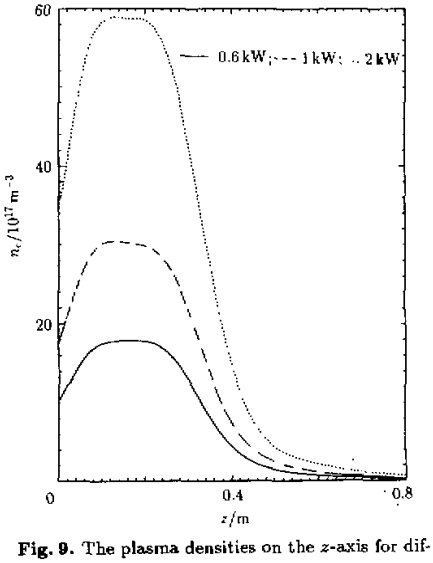

Fig. 9. The plasma densities on the z-axis for different power inputs at p = 1 mTorr.

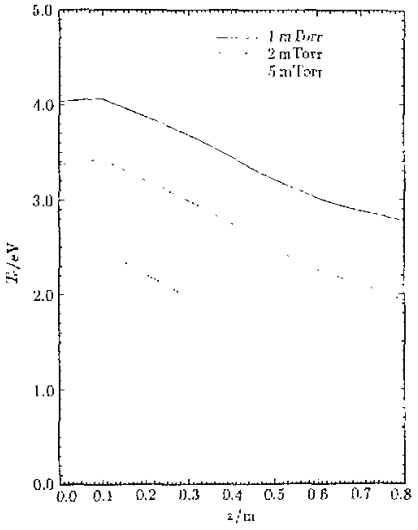

Fig. 10. The electron temperatures on z-axis for different neutral gas pressures at $p = 0.6$ kW.

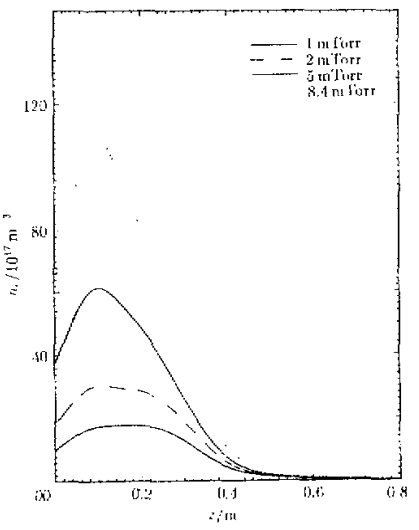

Fig. 11. The plasma densities on z-axis for different neutral gas pressures at $p = 0.6$ kW.

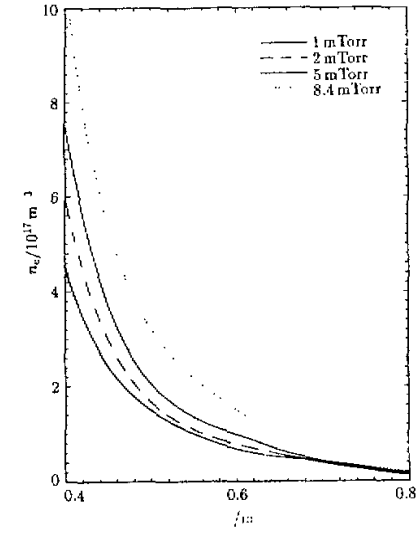

Fig. 12. The plasma densities on z-axis in downstream area for different neutral gas pressures at $p = 0.6$ kW.

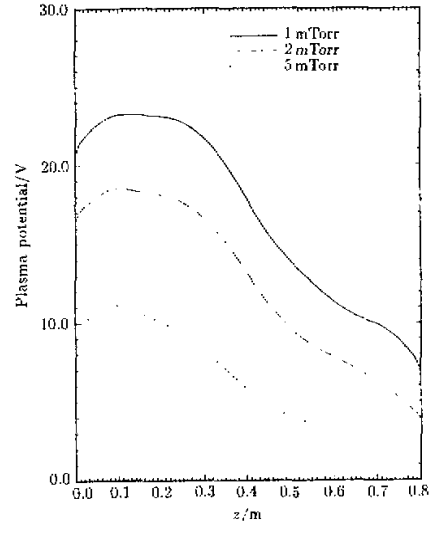

Fig. 13. The plasma potential on z-axis for different neutral gas pressures at $p = 0.6$ kW.

The curves shown in Fig. 6 are the energy distributions for those ions impacting on the wafer at the bottom of the chamber for various annular radial positions. Since the plasma density and the potential near the center ($r \to 0$) are higher than those near the edge

($r \to 30$ cm), the energy flux at the center is larger than those far away from the center. It obviously depends primarily on the plasma potential near the sheath. In order to find the function of the power input, three power inputs are considered here, i.e., $P = 0.6$, 1 and 2 kW. The neutral gas pressure is 1 mTorr for all these cases. For convenience of comparison, 1-D plots are adopted here. Figure 7 shows that the electron temperature difference among those different power inputs is too small to recognize, especially in the downstream area. Even near the resonant zone, the difference between T_e (2 kW) and T_e (0.6 kW) is only 3%. It implies that most of the microwave power do not go for the electron temperature increasing. Though the experimental results show that there is still a little difference for different input powers[2], the difference seems not so significant. Figure 8 gives the similar conclusion, which means the power input does not affect the potential too much. Now let us find where the main part of the microwave power would go. From Fig. 9, it can be seen that the plasma density is apparently dependent on the power input when the neutral gas pressure is a constant. It seems that the densities, in both source and downstream areas, are almost proportional to the power input to a certain extent. The main part of the power contributes to the ionization so that the plasma density bears proportion to the power input. These results seem to be in good agreement with the experimental measurements.[2,15] Our latest research has found the distribution of the power consumption for various physical processes, such as ionization, excitation, metastable excitation and energy flowing out of the chamber.[13]

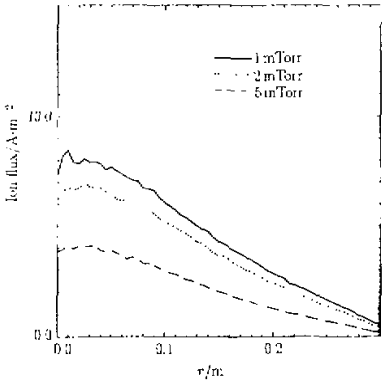

Fig. 14. The ion flux for different neutralgas pressure at $p = 0.6$ kW, $z = 0.8$ m.

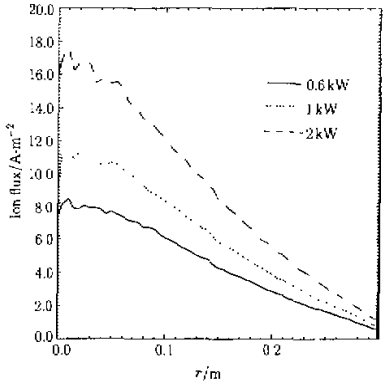

Fig. 15. The ion flux for different power inputs at $p = 1$ mTorr, $z = 0.8$ m.

From Fig. 10 through Fig. 12, we have the results of T_e, ϕ and n_e for different neutral gas pressures, i.e., $p = 1$, 2 and 5 mTorr. Figure 10 shows that the electron temperature is obviously affected by the neutral gas pressure. The higher the pressure, the lower the electron temperature would be. The explanation seems to be that the higher gas density would yield the higher electron neutral gas collision frequency that transports a great amount of energy from the electrons to the neutral gas, and in turn the higher inelastic collision frequency would result in the more strong ionization. Therefore, the plasma density is supposed to go up if the neutral gas pressure becomes large. By means of comparison with experimental measurements, it is found that the experimental results are slightly higher

than our simulation results.[2] The reason may be the numerical dissipation making the temperature lower. As to the relation between electron temperature T_e and neutral pressure p, the tendency agrees well with Refs. [2, 15], i.e., the higher the pressure, the lower the temperature. From Fig. 11, it can be seen that the plasma density becomes larger when the neutral gas pressure is increased. To see the difference clearly on the downstream, Fig. 12 is plotted from $z = 40$ to 80 cm in the downstream area. The results are qualitatively in good agreement with the experimental measurements.[2,15] Figure 13 shows the potential distributions along the z-axis. It is found that the potential becomes smaller when the pressure goes up, and a high gas pressure would result in a low potential but high plasma density. The reason may be that the plasma has to be primarily held by its potential if the collision frequency of electron-neutral gas is very low. If the pressure is increased and the collision frequency becomes high, the plasma can be no longer held only by the self-electric field. Instead, the high collision frequency prevents the plasma from escaping easily.

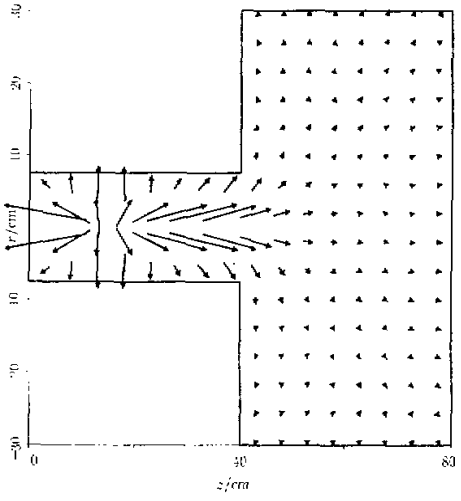

Fig. 16. The ion flux in the longitudinal cross section with $P = 0.6$ kW and $p = 1$ mTorr.

Some comparisons of ion fluxes between different pressures on the bottom, where the wafer is supposed to be held, are made in Fig. 14. It is found that the ion flux is the smallest when $p = 5$ mTorr, whereas the ion flux is the largest when $p = 1$ mTorr. Obviously, the lower neutral gas pressure would lead to the higher ion flux on the wafer, which implies that the appropriate low gas pressure may be helpful to increasing the etching rate. However, the ion flux uniformity in the higher pressure case seems better than that in the lower pressure case. In Fig. 15, there are the ion flux distributions for different power inputs. It is found that these ion flux distributions are partially dependent on the input power. The higher power input would lead to a higher ion flux impacting on the wafer, and this will probably result in the higher etching rate. Due to the numerical scheme, the volume cell $2\pi r\triangle r\triangle z$ near the center axis (z-axis) is too small to hold enough meta-ions. Therefore, poor statistics leads to the unexpected fluctuation like dips at the $r = 0$ points in Figs. 14 and 15. The ion flux in the longitudinal cross section of θ = constant is displayed in Fig.16. The ion flux

near the resonance zone in the source is much larger than that in the down stream. The flux decays rapidly as soon as the ions enter the downstream chamber.

IV. SUMMARY AND CONCLUSIONS

In this paper, a number of ECR argon plasma parameters in a typical extended apparatus are studied by means of numerical simulation method. Using the 2-D hybrid fluid-particle model, we have shown some relations between some parameters and the microwave input powers and the neutral gas pressures for Ar plasma. The major conclusion reached through our studies has shown that the hybrid model simulation of such discharges with realistic ratios of Debye length to discharge dimension scales works well and agrees with the previous experimental measurements reasonably.[2,15]

It is found that the input power does not significantly affect the plasma potential and the electron temperature. However, the plasma density seems directly influenced by the input power. It implies that the main part of the power goes for the inelastic ionization collision instead of raising the electron temperature. Meanwhile, the plasma potential can hardly be affected by the input power.

The neutral gas pressure plays an important role in both increasing the plasma density and decreasing the plasma potential. A higher pressure would result in a higher plasma density and a lower plasma potential. The electron temperature goes down when the pressure goes up.

Finally, the ion fluxes are examined. It is shown that the ion flux is also affected by both the gas pressure and the input power. It implies that the etching rate may be affected seriously by the gas pressure as well as the input power. Appropriately adding more power input and reducing the neutral gas pressure will probably improve the etching parameters significantly.

REFERENCES

[1] M. A. Lieberman and R. A. Gottscho, physics of Thin Films, edited by M. Francombe and J. Vossen (Academic Press, New York, 1993).

[2] S. M. Gorbatkin, L. A. Berry and J. B. Roberto *et al.*, *J. Vac. Sci. Technol.*, **A8** (1990), 2893.

[3] J. Asmussen, *J. Vac. Sci. Technol.*, **A7** (1989), 883.

[4] J. E. Stevens, Y. C. Huang, R. L. Jarecki and J. L. Cecchi (private communication, submmitted to *J. Vac. Sci. Technol.*).

[5] R. K. Porteous and D. B. Graves, *IEEE tran. Plasma Science*, **18** (1991), 204.

[6] J. L. Cecchi, J. E. Stevens, R. L. Jarechi, Jr and Y. C. Huang, *J. Vac. Sci. Technol*, **B9** (1991), 318.

[7] Peter H. Singer, Semiconductor International (July, 1991), p. 46.

[8] R. K. Porteous, H-M Wu and D. B. Graves, *Plasma Source and Technology*, **3** (1994), 25.

[9] Takashi Namura, Hiroyuki Okada, Yasushi Naitoh, *et al.*, *Japan. Appl. Phys.*, **29** (1990), 2251.

[10] Seiji Samukawa, Sumio Mori and Masami Sasaki, *Japan. J. Appl. Phys.*, **29** (1990), 792.

[11] Seiji Samukawa, *Japan. J. Appl. Phys.*, **29** (1990), 980.

[12] D. B. Graves, H-M Wu and R. K. Porteous, *Japan. J. Appl. Phys.*, **32** (Part 1, 6B) (1993), 2999.

[13] H-M Wu, D. B. Graves and R. K. Porteous, *Plasma Source and technology* (in press).

[14] N. D. Bowden *et al.*, *J. Appl. Phys.*, **73** (1993), 2732.

[15] R. A. Stewart *et al.*, Memorandum No. UCB/ERL M90/100, 12 November, 1990, Electronics Research Laboratory, College of Engineering, University of California at Berkeley, CA 94720, USA.